Kütahya Dumlupınar University
Institute of Graduate Studies

Journal of Scientific
Reports-A
E-ISSN: 2687-6167
Number 52, March 2023

RESEARCH ARTICLE

MINERALOGY AND GEOCHEMISTRY OF COAL-BEARING TUNÇBİLEK FORMATION İN THE TUNÇBİLEK-TAVŞANLI COALFIELD (KÜTAHYA, W-TURKEY)

Selin KARADİREK[1*]

[1,*]Akdeniz University, Faculty of Engineering, Department of Geological Engineering, Antalya, selinhokerek@akdeniz.edu.tr, ORCID: 0000-0003-4829-600X

Receive Date:21.10.2022 *Accepted Date: 22.01.2023*

ABSTRACT

Tunçbilek-Tavşanlı (Kütahya) Basin is among the most important Neogene coal deposits of Turkey. This study aims to determine the mineralogical and geochemical properties of the rocks (coal, roof, floor and parting) in the Tunçbilek-Tavşanlı coal field. The main abundant minerals in Tunçbilek-Tavşanlı coals are quartz, kaolinite, illite-smectite and siderite. Dolomite, illite, smectite, mica, feldspar, pyrite, chlorite and jarosite are less abundant minerals. The mineralogy of non-coal rocks is similar to that of coals, but pyrite is absent. The most abundant major oxides in the studied samples are SiO_2, Al_2O_3 and Fe_2O_3, respectively. The SiO_2, Al_2O_3 and MgO are the most abundant major oxides, respectively, in the claystone samples representing partings. Trace element concentrations of Tunçbilek-Tavşanlı coal samples mostly showed higher concentrations (excluding Ba, Sr, Pr, Tb, Dy, Ho, Tm, As, Cd and Bi) compared to the world low-rank coal average. According to the relative enrichment of the elements, the concentration coefficients (CC) of the coal samples are generally in the range of slightly enriched-normal; The CC of the non-coal samples mainly indicate the normal. The average REY concentration in the studied samples is higher than the world low-rank coal concentration and mostly showed L-type enrichment. Moreover, the REY concentration of the supercritical groups constitutes a significant part of the REY_{total} concentration in the samples taken from the coal horizon. However, the studied samples are in the unpromising area according to the low cut-off grade value and the relationship between cut-off grade-$C_{outl.}$ The high correlation coefficient between ash content and REY concentrations also indicates a mineral substance relationship. Al_2O_3/TiO_2 (between 12.5-31.7) ratios of Tunçbilek-Tavşanlı samples show intermediate and felsic source rocks.

Keywords: *Coal, REE+Y (REY), Trace elements, Tunçbilek*

1. INTRODUCTION

Coal, as an important energy source, consists of water, minerals, elements, rock fragments in addition to organic matter. Coal is still an important resource for many countries all around the world [1, 2]. Minerals and elements found in coal are more important than other side components. According to

numerous studies in this area, coal contains the greatest variety of minerals and elements existing in nature. From a scientific view of point, minerals and elements in coal are important parameters for determination of paleoenvironment-paleoclimate characteristics and geological evolution of coal, as they may include detailed records that occurred during peatification and subsequently changed during the coalification process [2-7].

Coal is used as an industrial raw material source in metallurgical processes, especially in electricity generation, in gasification, in cement industries, in the biological conversion process to high-value agricultural products. Furthermore, some coals contain Ge, Ga, U, V, Se, rare earth elements and Y (REE+Y or REY if Y is not included), some critical base metals such as Sc, Y, Au, Ag, Al and Mg [8]. Although the minerals and elements in coal are generally thought to have negative effects during the production, transportation and combustion of coal [9], they also have some beneficial aspects. Especially rare earth elements and some elements such as Y, Li, Ga, Se, Zr and Nb [8, 10-12] in coal attract attention as a potential raw material source, as they are used in the semiconductor industry. The concentrations of rare elements in coal ash are fairly high to make extraction in some countries [13-18]. Coals with high Al content have also attracted much attention in China in recent years because the coal ash has more than 50% wt. Al_2O_3 and has therefore been used for Al extraction [19, 20].

The Kütahya basin is an important basin with a variety of mineral deposits. There are also important coal deposits in the Tunçbilek-Tavşanlı basin. The first detailed geological study in the region was carried out by Arni in 1942 [21]. Afterwards, various studies on geology, tectonism and sedimentology of the basin have been carried out by many researchers [22-32]. With the understanding of the existence of economically important mineral deposits in the basin, studies have begun to be detailed in this direction [33-45]. This study is aimed to determine the major-trace element geochemistry and mineralogical composition of the coals and roof, parting, and floor associated with coal in the Tunçbilek coalfield, located in the west of Turkey, and to examine the usability as a by-product raw material in the industrial field based on these data.

2. GEOLOGICAL EVOLUTION AND STRATIGRAPHY OF THE STUDY AREA

The tectonic units forming the Anatolian plate were named by Ketin (1966) [46] for the first time as the Pontides in the north, Anatolides, Taurides and Border Folds towards the south. In later studies, it was distinguished from north to south as Rhodope-Istranca Zone, Istanbul Zone, Sakarya Zone, Anatolide-Tauride block (Tavşanlı Zone, Afyon Zone, Menderes Massif) Kırşehir Massif, Arabian Platform by Okay and Tüysüz (1999) [47]. Figure 1 shows the location of study area that is placed in the north of Tunçbilek in Tavşanlı-Kütahya district.

Western Anatolia, in which the study area is located, contains several tectonostratigraphic units (Sakarya Zone and Anatolide-Tauride Block) from northern to southern [47, 48]. Around the study area, the Anatolide-Tauride Block consists of the Menderes Extensional Core Complex representing the metamorphic massif [49], the Afyon Zone metamorphic rocks [50] and the mélange units of the İzmir-Ankara Zone [51], together with the ophiolites and blueschist facies of the Tavşanlı Zone [39, 52]. The blueschist facies of the Tavşanlı Zone represent the Anatolide-Tauride Block subducting towards the north, under the Sakarya Zone during the Cretaceous-Paleocene [53]. Eocene-Oligocene

sedimentary units unconformably overlie these tectonic units [39]. All these units are covered by Neogene sedimentary units. E-W trending grabens (such as Bakırçay, Kütahya, Gediz, Simav, Küçük Menderes, Büyük Menderes) and NE-SW trending basins (such as Gördes, [54], Selendi [55], Emet [56], Uşak-Güre [57], Tunçbilek-Domaniç [22, 26, 58] and Seyitömer basins [26, 59]) in Western Anatolia are the basins that developed due to the extensional tectonic regime. The Kütahya Graben, which is divided into sub-basins namely Tavşanlı and Seyitömer. Tunçbilek-Tavşanlı coalfield is placed in Tavşanlı sub-basin [45].

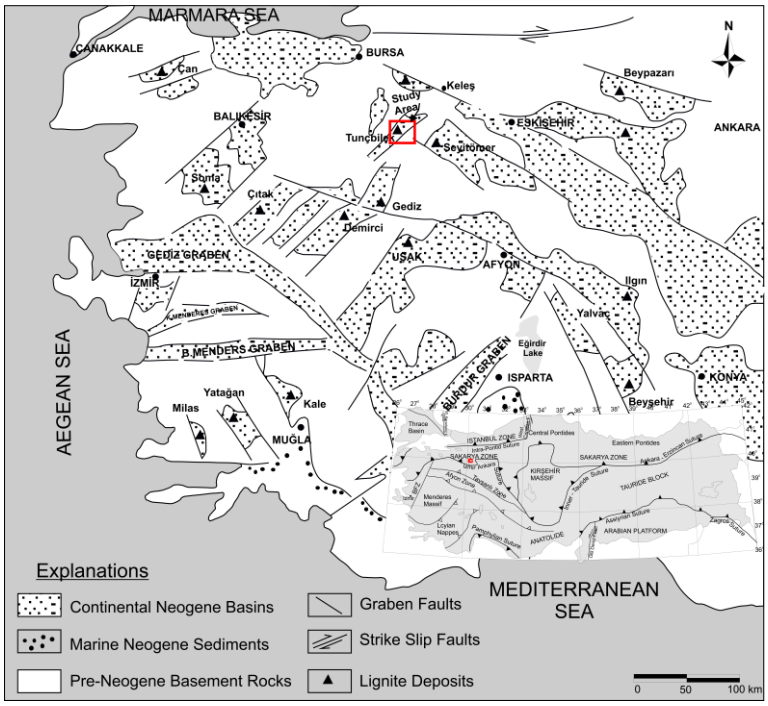

Figure 1. Tectonic setting of the Western Anatolian Neogene basin and location map of the study area (modified from [60] and [47]).

The basement rocks of the study area consist of metamorphic and ophiolitic rocks represented by Paleozoic and Mesozoic schist, quartzite, marble, serpentinite, peridotite, metaclastics and metacarbonates [26, 45]. In addition to other basement rock types, Eocene aged limestones (Oğulcaktepe Formation) exhibit a limited distribution [26, 39] (Fig. 2 and 3).

Beke Formation units (conglomerate, sandstone, claystone) are overlain on the basement rocks in Miocene. Baş (1986) [26] determined the age of Beke Formation as Middle Miocene based on pollen analysis. The coal-bearing Miocene Tunçbilek Formation, consisting of three members (Demirbilek, Gürağaç and Yeldeğirmeni, respectively) is unconformably overlain on the Beke Formation. The Tunçbilek Formation shows lacustrine conditions. Demirbilek member of Tunçbilek formation

represents the coal-bearing marl, sandstone, and claystone. The Gürağaç member, which is gradually overlain by conglomerate, sandstone, and claystone intercalations, overlies the Demirbilek member, and the Tunçbilek Formation ends with the clayey-silicified limestones of the Yeldeğirmeni Member overlying the Gürağaç member [26, 39]. Common pyroclastic rocks in the basin are called Civanadagi tuffs [26].

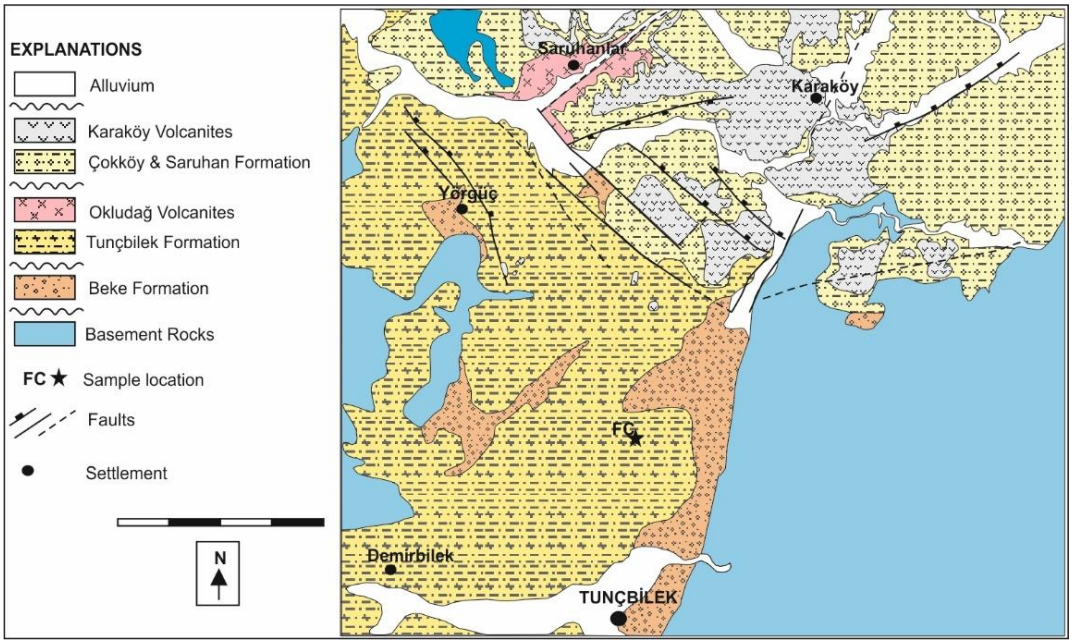

Figure 2. Geological map of the Tunçbilek-Tavşanlı basin (modified from [26], [39], [58] and [61]).

The Civanadağ tuffs conformably overlie the Tunçbilek Formation and are interbedded with the Oklukdağ Volcanites consisting of dyke, dome and lava flows [26]. The Saruhanlar Formation include conglomerate, sandstone, limestone and tuff layers and they are unconformably overlain on the Tunçbilek Formation during the Pliocene. Saruhanlar Formation is covered by andesitic-basaltic rocks called Pliocene Karaköy Volcanics and is vertically transitional to Çokköy Formation. The Çokköy Formation consists of conglomerate, claystone and marl. Due to the uplift and evaporation processes of the region in the Upper Pliocene, the lacustrine environment conditions have ended. The deposits overlying the Pliocene units are represented by Quaternary coarse-grained clastics, and travertines [26].

3. MATERIAL AND METHOD

The field studies were carried out in the open pit FC panel of the Garp Lignites Enterprise located in the Tunçbilek coal basin. Samples (total 25 samples including coal, clayey coal, carbonaceous shale,

and claystone) were taken from the open pit mine along the coal seam profile using the channel and representative sampling method.

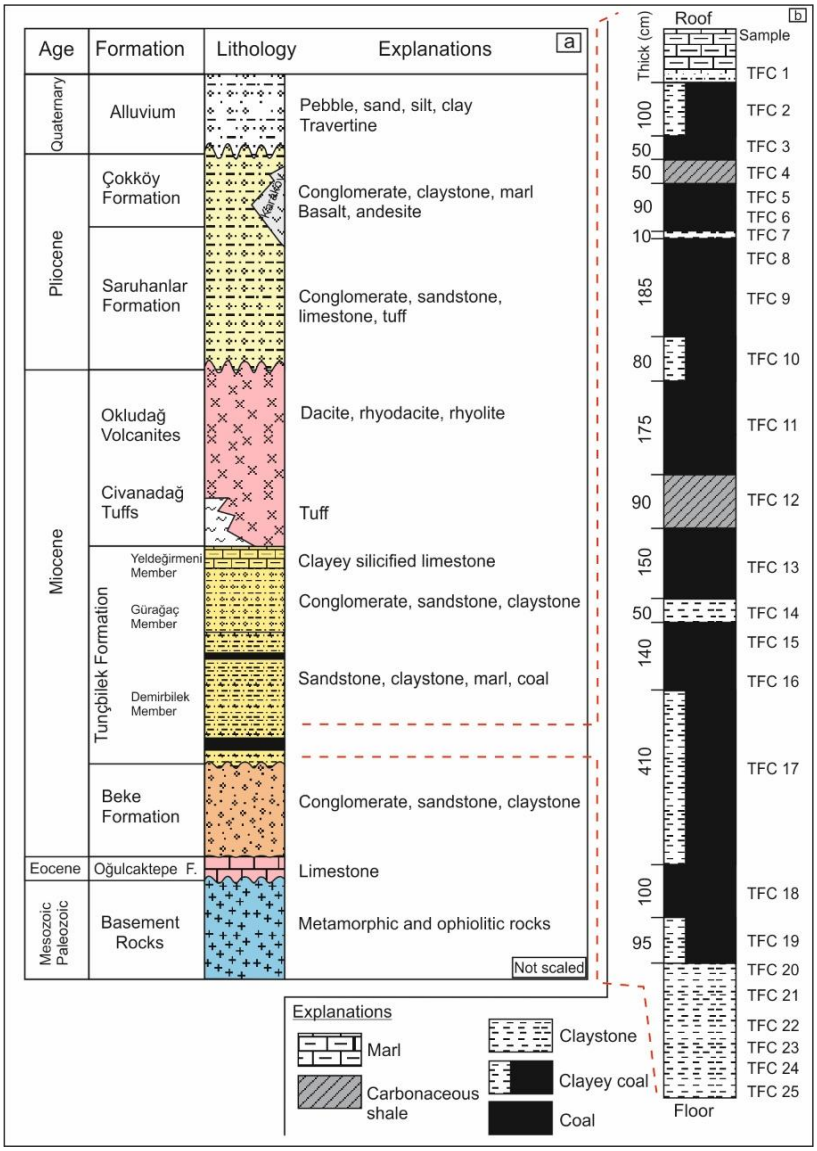

Figure 3. a) Stratigraphic column of Tunçbilek-Tavşanlı basin (modified from [26] and [39] b) Coal seam profile of FC panel open pit.

Major and trace elements concentrations were determined using ICP-MS and ICP-AES at ACME Analytical Labs (Canada). Some trace elements such as Ni and Sc, and major oxide elements were determined by ICP-AES using $LiBO_2$ fusion method. Some of trace elements (Ba, Be, Co, Th, U, Sn,V) were determined by ICP-MS. Samples were decomposed by fusion with $LiBO_2$ before determining the total amounts of the elements. Other trace elements were also determined by ICP-MS based on the analysis of solutions (10 ml diluted fraction) obtained from 0.5 g samples.

There are some methods for detecting and identifying minerals in whole rock. Batch chemical analysis provides clues as to which minerals or mineral groups might be present in the sample. The mineralogical properties of the samples were determined by X-ray diffraction (XRD) analysis at the General Directorate of Mineral Research and Exploration (MTA) laboratory (Ankara, Turkey) using the Rigaku Geigerflex D-MaxII device. XRD analyzes were performed using copper [λ(CuKα) = 1.54056Å] radiation at scan rates of 2θ=2-70° per minute and 0.01°/minute. Samples for clay analyzes were prepared by separating the clay fraction using settling and centrifuging the suspension after dispersing in distilled water overnight. Clay particles were dispersed using ultrasonic vibration for about 15 minutes. Oriented samples of <2 µm fractions from each sample were prepared for analysis with normal spinning with air drying in the range of 2-30º 2θ, with ethylene-glycol in the range of 2-20 2º, with dissolving at 60 °C for 2 hours, and with heating at 550 °C for 2 hours in the range of 2-15 2º. Mineral definitions on the obtained diffractoms were made using ASTM cards.

4. RESULTS AND DISCUSSION

4.1. Mineralogical Composition

The mineralogical composition of the samples determined by XRD whole rock and clay fraction analysis is given in Table 1. The non-clay minerals are, in order of abundance, quartz, siderite, dolomite, mica, K-feldspar, pyrite, and jarosite (Fig. 4). Since most of the samples examined are coal, organic materials are also present. Other samples are roof, floor and parting samples. The clay minerals are kaolinite, illite-smectite, illite, smectite, and chlorite (Fig. 5). It has been stated that quartz exhibits a distinct behavior at the time of coal formation as it has no significant relationship with other minerals and is predominantly of detrital origin [62]. However, it is rarely an authigenic (especially epigenetic) mineral in coal. [63]. Considering the previous studies, in the samples examined, it was determined that quartz was of clastic origin; it is thought to be originated from basement rocks (metamorphic) and volcanic materials. Epigenetic carbonate minerals (ankerite, calcite, dolomite, siderite) are commonly found as joint infillings in coal seams [64]. Cicioglu Sutcu et al. (2021) [45] determined that dolomite and siderite minerals in Tunçbilek coals are of syngenetic and epigenetic origin. Dolomite, siderite and calcite (only in one sample) minerals were detected in the examined samples. (Table 1).

The most abundant mineral in altered volcanic ash in coal horizon is kaolinite. However, an important amount of other clay minerals can exist in some cases [65]. Less stable primary minerals and alteration of volcanic glass can lead to the formation of kaolinite, smectite, illite, illite-smectite and chlorite [65] and may be transported into the basin by streams [24, 26, 66, 67]. The dominant clay minerals in the studied samples are kaolinite and illite-smectite. The accumulation of volcanogenic material in the peat bog environment of the Tunçbilek basin is formed by the transformation of

feldspar and mica group minerals into kaolinite and volcanic ash into tonsteins and overlain by coal seams in the basin [32].

Table 1. Mineral compositions of Tunçbilek-Tavşanlı samples (+++ dominant (>20%), ++ abundant (5-20%), + minor (<5%), Carb. shale : Carbonaceous shale).

Lithology	Sample No	Quartz	Dolomite	Siderite	Calcite	K-Felds.	Mica	Pyrite	Jarosite	Kaolinite	Chlorite	Illite	Illite-Sm.	Smectite
Claystone	TFC1	+++		++		+	+	+		+		++	+	
Clayey coal	TFC2	+++	+	++		+	+	+		++		++	+	
Coal	TFC3	++	++	+			+	+		++		+	+	+
Carb. shale	TFC4	+++	+	+	+		+	+		++		+	+	
Coal	TFC5	+++		+			+	+		++		+	+	
Coal	TFC6	++		+		+	+	+	+	++		+	+	
Claystone	TFC7	+++	+	+		+	+	+		++			++	+
Coal	TFC8	+++		+			+			++		+	+	
Coal	TFC9	+++		+		+	+			++		+	+	
Coal	TFC10	+++		+		+	+			++		+	+	+
Coal	TFC11	++	+	+			+	+	+	++	+		++	
Carb. shale	TFC12	+++	+	+			+	+	+	+++	+	+	+	
Coal	TFC13	++		+			+	+		++	+		+	
Claystone	TFC14	+++	+	++			+			++			+	
Coal	TFC15	+++		+			+		+	++			++	
Coal	TFC16	++	++	+			+			++		+	++	+
Clayey coal	TFC17	+++	+	+			+	+	+	+		+	+	
Coal	TFC18	++		+			+	+		++		+	++	
Coal	TFC19	++	+	+			+	+		++		+	+	
Claystone	TFC20	+++		+		+	+			++		++	+	
Claystone	TFC21	+++		+			+		+	++		++	+	
Claystone	TFC22	+++		+			+			++	+	++	+	
Claystone	TFC23	+++	+	++		+	+			+++	+	++	+	
Claystone	TFC24	+++	+	+						++		+	+	
Claystone	TFC25	+++	++	+			+			++		+	+	

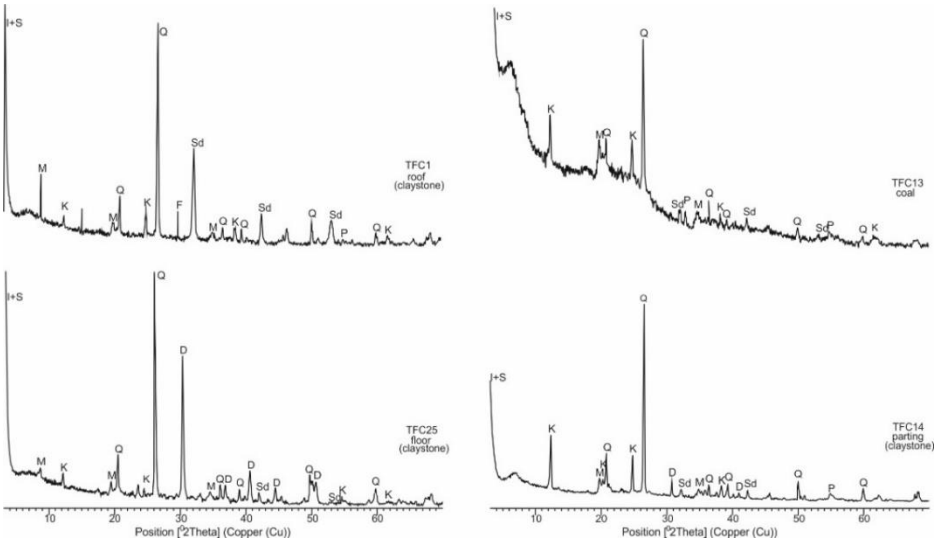

Figure 4. XRD patterns of specific samples. S= smectite, I= illite, K= kaolinite, M= mica, Q= quartz, D= dolomite, Sd= siderite, P= pyrite.

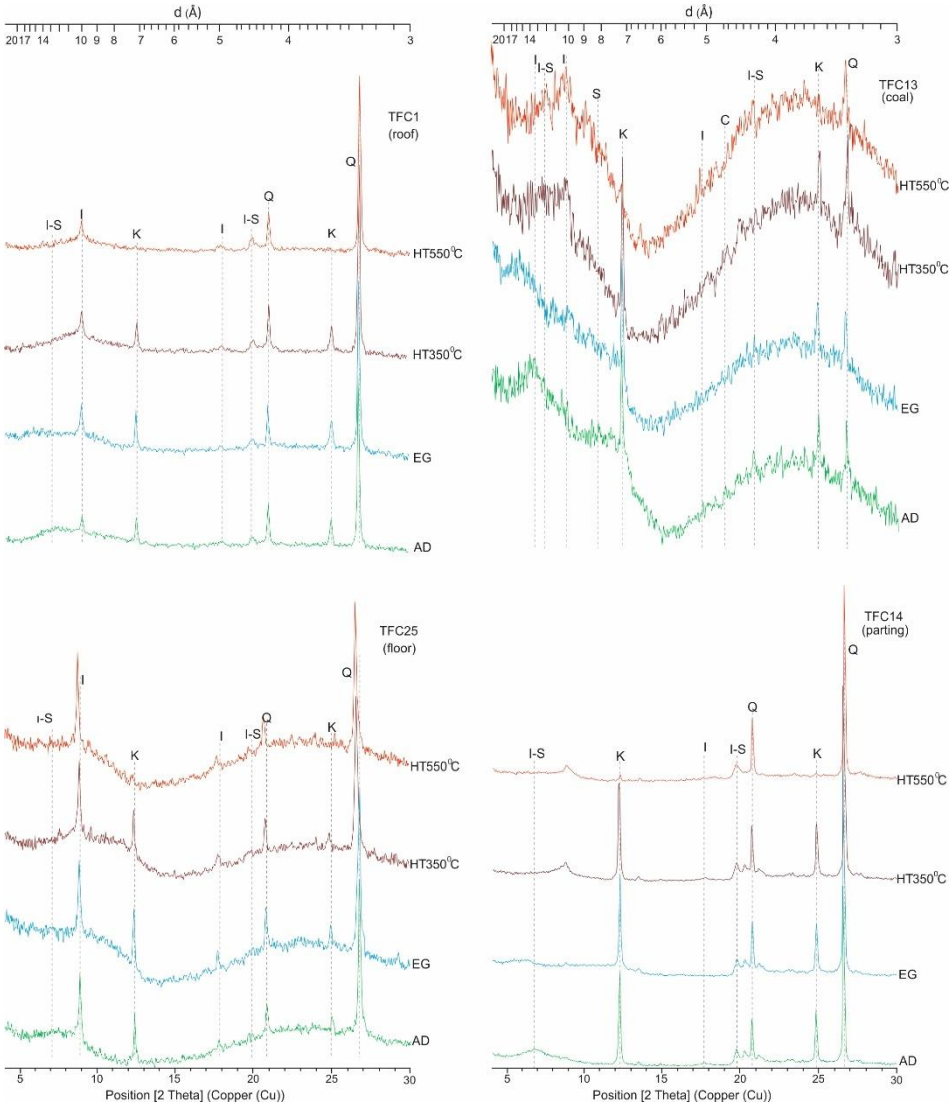

Figure 5. Detailed XRD patterns of specific samples. S= smectite, I= illite, K= kaolinite, Q= quartz, C= chlorite.

4.2. Chemical Composition

4.2.1. Major oxide elements

The concentrations of major oxides in the coal seam profile (coal, roof, parting, and floor) samples and the average values for world low-rank coals are given in Table 2. SiO_2, Al_2O_3 and Fe_2O_3 were found to be the most abundant major oxides in samples of coal, carbonaceous shale, and claystone

representing the roof and floor (except TFC24 and TFC25), whereas MgO, K_2O, CaO, TiO_2, Na_2O, P_2O_5 and MnO were found in smaller amounts. SiO_2, Al_2O_3 and MgO are the most abundant major oxides in the parting samples, while Fe_2O_3, K_2O, TiO_2, CaO, P_2O_5, Na_2O and MnO major oxides are present in smaller amounts. Major oxides are high in claystone and carbonaceous shale layers of profile samples. Concentrations of SiO_2 and Al_2O_3 in coal samples are quite low compared to other samples (Table 2).

Table 2. Major oxide and ash contents of FC panel samples of Tunçbilek-Tavşanlı.

Samples	SiO_2	Al_2O_3	Fe_2O_3	MgO	CaO	Na_2O	K_2O	TiO_2	P_2O_5	MnO	LOI	Al_2O_3/TiO_2	Ash
	%												
TFC1	47.43	11.31	10.66	5.13	1.00	0.08	1.25	0.62	0.12	0.24	21.7	18.2	80.0
TFC2	41.88	13.83	4.94	3.07	0.77	0.09	1.37	0.62	0.15	0.08	32.8	22.3	64.0
TFC3	6.36	2.52	1.65	0.95	0.97	0.00	0.15	0.11	0.00	0.03	87.2	22.9	19.5
TFC4	68.16	11.90	2.81	2.05	0.22	0.03	0.72	0.53	0.05	0.02	13.4	22.5	86.5
TFC5	34.93	5.20	0.78	0.58	0.14	0.02	0.27	0.29	0.03	0.00	57.6	17.9	28.6
TFC6	11.88	3.78	2.27	0.95	0.83	0.00	0.18	0.17	0.01	0.00	79.8	22.2	26.2
TFC7	48.05	26.29	2.45	3.18	0.31	0.06	0.86	0.83	0.21	0.00	17.3	31.7	83.2
TFC8	38.63	15.25	2.76	1.73	0.21	0.03	0.81	0.60	0.03	0.02	39.7	25.4	30.8
TFC9	27.34	9.82	2.86	1.57	0.38	0.02	0.65	0.44	0.02	0.02	56.6	22.3	40.9
TFC10	39.91	16.18	3.14	2.30	0.19	0.02	1.11	0.73	0.04	0.03	35.9	22.2	32.9
TFC11	25.83	11.00	3.06	1.50	0.19	0.02	0.66	0.41	0.04	0.02	57.0	26.8	15.6
TFC12	59.90	21.89	1.38	1.61	0.73	0.05	1.00	0.78	0.20	0.01	12.1	28.1	88.1
TFC13	11.27	4.41	2.97	0.74	0.19	0.01	0.30	0.25	0.03	0.02	79.6	17.6	12.6
TFC14	53.12	19.46	4.07	4.33	1.24	0.05	0.84	0.77	0.23	0.07	15.4	25.3	86.0
TFC15	49.61	17.63	4.77	3.27	0.46	0.03	1.57	0.90	0.22	0.05	20.9	19.6	52.8
TFC16	12.77	3.45	2.38	3.60	5.35	0.02	0.21	0.25	0.02	0.06	71.6	13.8	35.6
TFC17	36.30	13.15	3.81	2.57	0.31	0.03	1.10	0.65	0.09	0.04	41.4	20.2	66.8
TFC18	4.76	2.08	1.08	0.19	0.03	0.01	0.12	0.10	0.00	0.00	91.5	20.8	10.5
TFC19	6.37	2.26	0.68	0.28	0.12	0.01	0.15	0.12	0.00	0.00	90.0	18.8	8.2
TFC20	66.21	13.46	3.76	2.30	0.67	0.20	2.08	0.65	0.19	0.16	9.9	20.7	87.4
TFC21	66.43	13.09	3.70	2.24	0.95	0.20	2.01	0.62	0.18	0.13	10.0	21.1	90.8
TFC23	34.59	11.53	16.27	7.24	4.66	0.06	1.39	0.92	0.26	0.54	21.9	12.5	89.7
TFC24	65.79	2.95	7.33	6.52	0.55	0.06	0.31	0.16	0.06	0.56	15.5	18.4	90.5
TFC25	39.64	6.89	6.55	8.12	12.51	0.08	1.05	0.41	0.19	0.19	24.0	16.8	90.1

Contents of SiO_2 vary between 49.61% and 4.76% in coal samples and 17.63% and 2.08% in other samples. Similarly, contents of Al_2O_3 range from 17.63% to 2.08% in coal samples and from 26.29% to 6.89% in other samples. Samples with high Al_2O_3 content are rich in kaolinite. Fe_2O_3 concentration is more abundant in the other samples compared to the samples belonging to the partings (Table 2). Siderite and pyrite minerals are relatively abundant in the mineralogical composition of these samples. Samples with high MgO content are those abundant in dolomite minerals (Table 1). There is a positive correlation between major oxides (Table 3). Al_2O_3 shows high positive linear correlation with SiO_2, K_2O, TiO_2, P_2O_5,and MgO exhibits high positive correlation with Fe_2O_3, CaO and MnO and (Fig. 6) Silicates are the most abundant mineral group in coal. Silicate group minerals are associated with many elements found in coal, particularly SiO_2, Al_2O_3, and to a lesser extent MgO, K_2O, TiO and clastic minerals such as major oxides, quartz, and clay, including Na_2O, CaO and Fe_2O_3, indicating a mixed clay assemblage [7, 68]. Other important silicates are micas, analcime and various feldspars [69]. The origins of SiO_2 and Al_2O_3 in the examined samples are kaolinite and illite-smectite mixed bedded clays. Concentration of SiO_2 is partially related to quartz content (Table 1).

Table 3. Ash contents (wt.%, db) and element affinities calculated from Pearson correlation coefficients (correlation is significant at 0.01, correlation is significant at 0.05 "*").

Correlation with ash (0.70 <r<1.0)	Ba, SiO_2, MgO, P_2O_5
Correlation with ash (0.50 <r<0.69)	Ga, Sr, Ta, Th, U, Cu, Pb, Zn, V, Y, Eu, Gd, Tb, Dy, Ho, Er, Tm, Yb, Lu, Al_2O_3, Fe_2O_3, Na_2O, K_2O, TiO_2, MnO
Correlation with ash (0.49 <r<0.20)	Ni, Sc, Co, Cs, Hf, Nb, Sn, W, Zr, Rb, La, Ce, Pr, Nd, Sm, Cd, Bi, Sb, Cr, CaO
Negative correlation with ash (-0.90 <r< -0.4)	Mo
Correlation with SiO_2	Ba, Cs, Ga, Rb, Ta, V, Y, La*, Ce*, Pr*, Nd*, Sm*, Eu*, Gd*, Tb*, Dy*, Ho*, Er, Tm, Yb, Lu, Pb*, Zn,Cd*, Bi*, Au
Correlation with Al_2O_3 0.5 <r<1.0	SiO_2, MgO, K_2O, TiO_2, P_2O_5, REE+Y (Y, La, Ce*, Pr, Nd, Sm, Eu, Gd, Tb, Dy, Ho, Er, Tm, Yb, Lu), Ba, Cs*, Ga, Hf, Rb, Sn, Sr, Ta, U, V, W, Zr, Pb, Zn, Bi, Au
Correlation with Fe_2O_3 0.5 <r<1.0	MgO, K_2O*, TiO_2*, MnO
Correlation with CaO	MgO (0.688)
Correlation with K_2O 0.5 <r<1.0	SiO_2, P_2O_5*
Correlation with TiO_2	SiO_2, Al_2O_3, Fe_2O_3*, K_2O, P_2O_5, REE+Y
Correlation with MgO 0.5 <r<1.0	Fe_2O_3, CaO, P_2O_5*
Correlation with Na_2O 0.45 <r<1.0	SiO_2, K_2O, P_2O_5*
Negative correlation with TOTC	Al_2O_3, SiO_2
Negative correlation with TOTS	SiO_2*

Samples containing abundant illite, illite-smectite and partially mica or feldspar have high K_2O concentration (Tables 1, 2). The source of MgO in low-rank coals is usually organic origin, calcite, and silicate minerals [70]. The source of MgO in the samples examined is dolomite, smectite and smectite-illite minerals. The source of Fe_2O_3 and CaO is usually dolomite, siderite, smectite and pyrite. MnO presented a positive correlation with MgO and Fe_2O_3 (Table 3). Therefore, MnO may be

of siderite origin. TiO_2, P_2O_5 and NaO, which are less abundant in the samples, may be derived from clay and mica group minerals [45, 70]. The ratio of Al_2O_3/TiO_2 is stated to be a reliable indicator for the provenance of sedimentary rocks [71, 72, 73, 74]. The ratios of Al_2O_3/TiO_2 are 3-8, 8-21 and 21-70 for sediments derived from mafic, intermediate and felsic igneous rocks, respectively [71]. The ratios of Al_2O_3/TiO_2 of Tunçbilek-Tavşanlı samples vary between 12.5-31.7 (Table 2), showing intermediate- felsic rocks. The tuffs in the study area have been characterized as rhyolitic-rhyodacitic tuffs [32].

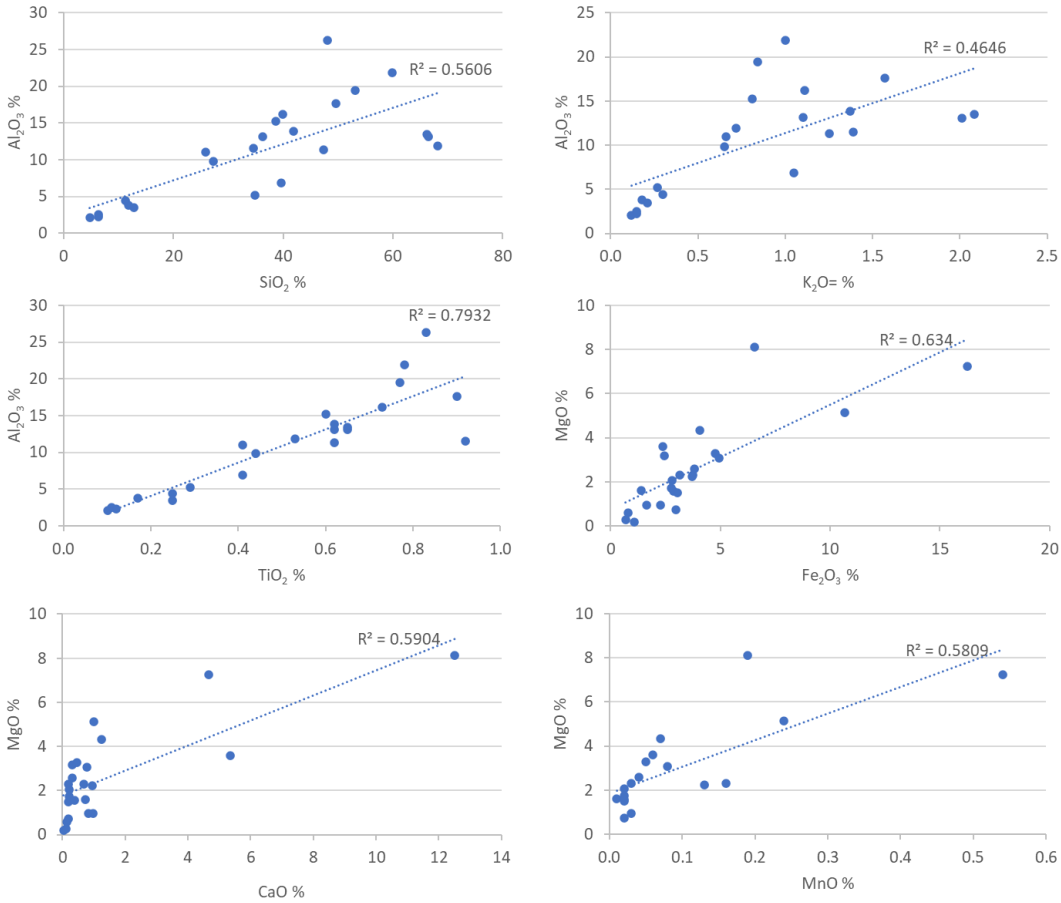

Figure 6. Plots showing relationship between some major oxides in all samples.

4.2.2. Trace elements

In this study, trace element values determined for studied coal samples were compared with the average values of world low-rank coals stated by Ketris and Yudovich (2009) [75] (Table 4). In the studied coal samples, Ni, Sc, Be, Co, Cs, Ga, Hf, Nb, Rb, Sn, Ta, Th, U, V, W, Zr, Y, La, Ce, Nd, Sm,

Eu, Gd, Mo, Cu, Pb, Zn and Hg elements presented higher concentrations compared to the world low-rank coal averages. The relative enrichment of trace elements is classified by Dai et al (2015a) [76]: "unusually enriched (CC >100), significantly enriched (10 < CC < 100), enriched (5 < CC < 10), slightly enriched (2 < CC < 5), normal (0.5 < CC < 2) and depleted (CC < 0.5)", where CC stands for concentration coefficient and is defined as the ratio of the concentration of trace elements in the samples studied to those in world coals). The CCs of studied coal samples are generally in the slightly enriched-normal range (Fig. 7a), whereas a normal enrichment (0.5 < CC < 2) is indicated according to the CC values of the non-coal samples (Fig. 7b).

Concentration of Ni (190–1960 µg/g, average 840 µg/g) in the samples of the Tunçbilek-Tavşanlı coal seam is much higher than the average value of world low-rank coals (9 µg/g; [75]) (Table 4) and concentration coefficients are much higher than 10 (CC >10) (Fig. 7a). Finkelman (1981) [77] stated that significant amounts of Ni in coal may be organically related. Inorganically bound Ni can be largely associated with sulfides. Finkelman (1988) [78] stated that Ni in coal can also occur in clays. Finkelman (1994) [79] noted a low level of confidence in Ni formation patterns due to the lack of direct evidence and the contradictory available evidence. In the studied samples, Ni showed a weak positive correlation coefficient with ash (Table 3). Therefore, considering the lithology of the source region, which gives detritus to the coal-bearing succession, rocks such as serpentine and peridotite found in the basement rocks may be responsible for the enrichment of Ni. Trace elements with a CC of 5-10 include Cs, Co and Rb. The Cs concentrations in the Tunçbilek-Tavşanlı coal seam vary between 1.10 and 9.20 µg/g. The weighted average of the Cs concentrations (5.25 µg/g) are higher than the world's low-rank coals (0.98 µg/g; [75]). Cesium is predominantly associated with silicate minerals in low-rank coals [70]. Cobalt is enriched in the Tunçbilek-Tavşanlı coal seam with a concentration ranging from 4.8 to 96.7 µg/g. The average Co concentration of 41.4 µg/g in the studied samples is much higher than the average Co concentration of the world's low-rank coals (4.2 µg/g) [75].

Cobalt in coal deposits generally occurs worldwide in an organic association or in Co-including minerals such as monosulfide, clay, and pyrite [70, 76]. Rubidium concentration in the studied samples ranges from 10.2 to 104.7 µg/g, presenting higher values compared to the average of world's low-rank coal and is associated with clay minerals (especially illite and mixed-layer clays). There is a weak positive correlation between Ce, Co and Rb and ash (Table 3) and shows the inorganic association. A series of trace elements including, Sc, Be, Hf, Nb, Ta, Th, V, W, Zr, Cu, Pb and Zn, are slightly enriched in Tunçbilek-Tavşanlı coals with CC values between 2 and 5. While Cd and Bi elements with concentration coefficients lower than 0.5 show depletion, other elements with CC from 0.5 to 2 have concentrations close to the world's low-rank coals average values.

Trace element concentrations of Tunçbilek-Tavşanlı coals present higher values for Ni, Co, Cs, Ga, Nb, Rb, Th, U, V, W, Zr, Cu, Pb and Hg elements comparing to USA and China coals. Moreover, Hf, Ta, Y and rare earth elements (REE) show higher concentrations than the USA coals. Compared to Chinese coals, the element As presents a higher concentration.

Parting, roof and floor samples, when compared with mean values for upper continental crust (UCC), only Ni (CC > 10) is significantly enriched element whereas Co, Th, U, Pb, As, Bi and Hg are slightly

enriched with CC between 2 and 5) (Fig. 7b). Moreover, the rest of trace elements have values close to the UCC averages with a concentration coefficient between 0.5 and 2.

JSR A
Journal of Scientific Reports

Table 4. Trace elements concentrations (µg/g) and the loss on ignition (LOI, %) of Tunçbilek-Tavşanlı samples.

Sample	TFC1	TFC2	TFC3	TFC4	TFC5	TFC6	TFC7	TFC8	TFC9	TFC10	TFC11	TFC12	TFC13	TFC14	TFC15	TFC16	TFC17	TFC18	TFC19	TFC20	TFC21	TFC23	TFC24	TFC25	World [75]	Lignite [75]	UCC [80]	USA [81]	China [3,6,82]
LOI	21.7	32.8	87.2	13.4	57.6	79.8	17.3	39.7	56.6	35.9	57	12.1	79.6	15.4	20.9	71.6	41.4	91.5	90	9.9	10	21.9	15.5	24	-	-	-	-	-
Be	3	6	1	3	5	4	4	7	2	2	2	2	1	6	2	9	2	2	1	2	2	2	1	1	1.6	1.2	2.1	2.2	2.1
Sc	17	15	4	8	5	6	2	12	11	15	7	8	5	6	14	7	13	5	4	16	14	23	7	11	3.9	4.1	14	4.2	4.4
V	107	124	24	49	70	41	104	103	81	90	48	98	40	104	92	101	92	40	23	127	123	123	38	75	25	22	97	22	35
Cr	0.08	0.05	0.02	0.03	0.02	0.02	0	0.04	0.06	0.07	0.04	0.02	0.03	0.02	0.09	0.03	0.07	0.02	0.01	0.05	0.05	0.09	0.02	0.04	17	15	0.01	0.001	-
Co	101	64.9	18.6	13.2	4.8	14	3	26.6	67.5	76.5	68	12.6	12.4	24.2	96.7	48.8	64.1	39.3	6.2	63.2	103.1	126.7	20.3	28.1	5.1	4.2	17.3	6.1	7.1
Ni	1335	1162	288	190	197	460	143	481	1064	1478	1128	199	638	367	1960	845	1923	477	309	914	1501	1477	316	505	13	9	47	14	13.7
Cu	60.7	75.3	10.7	29.2	16.7	13.5	9.4	50.7	33	61.7	42.2	22.7	29.6	22.5	63.3	34.5	55.7	26.5	11.6	53.2	60.5	89.9	16.9	32.7	46	15	28	16	17.5
Zn	88	79	14	38	16	22	107	48	43	78	66	106	22	96	62	25	43	11	18	98	87	77	18	41	23	18	67	53	41.4
Ga	13.4	15.5	2.2	14.8	6.7	4.6	25.9	15.3	10	17.1	9.9	22	4.5	20.1	18.9	4.5	14.2	2	2.3	15.5	15.4	12.1	3	8	5.8	5.5	17.5	5.7	6.6
As	47.6	8	3.2	0.8	1.7	10.7	4.8	2.1	4.1	1.9	32.1	2.1	3.8	4.1	2.6	6.5	1.8	2.9	6.2	10.2	18.6	29.1	27.9	10.7	8.3	7.6	4.8	24	3.8
Rb	66.9	78.1	10.2	63.3	23.8	14.1	25.4	87.2	74.7	94.2	57.4	53.9	20.2	37.3	104.7	15.3	86.3	9.3	9.2	90.3	88.6	53.9	14.3	44.8	14	10	84	21	9.3
Sr	83.7	113	31.7	85.6	65.7	55.4	815.2	97.2	62.8	94.6	84.1	435.1	110.1	550.1	125.9	75.8	101.5	16.4	25.3	243.4	188.7	302.9	33	150.2	110	120	320	130	140
Zr	118.3	154.1	29	153.4	385.9	141.2	520.8	151.2	142.1	136.4	69.6	245.8	48.7	356.1	136.9	103.6	143.7	73.1	30.5	115.1	99.6	137.1	33.5	64.1	36	35	193	27	89.5
Nb	14.3	12.9	2	22.6	39	9.9	12.8	16.6	10.1	15.3	5.1	13.1	4.3	19.4	23.2	16.9	11.5	3.2	3.1	11.8	11.3	17.4	3.4	7.7	3.7	3.3	12	2.9	9.4
Mo	1.1	3.7	2.6	0.4	2.5	3.5	1.4	3.1	2.9	1	4.6	0.4	1.6	2.4	1.2	6	1.3	3.3	1.3	0.5	0.4	0.7	0.8	0.4	2.2	2	1.1	3.3	3.1
Sn	1	2	1	2	1	1	6	2	1	3	2	7	1	5	3	1	2	1	1	2	2	1	1	1	1.1	0.79	2.1	1.3	2.11
Cs	7.9	8.4	1.9	8.1	3.5	1.9	3.6	9.2	6.2	8.9	6	6.1	3.4	2.6	8.9	2.4	7.3	1.1	1.5	9.1	8.9	4.2	2.2	10.3	1	0.98	4.9	1.1	1.13
Ba	208	183	21	114	63	31	387	123	78	103	65	378	139	306	234	34	495	14	19	468	437	211	204	217	150	150	624	170	159
Hf	3.3	3.5	0.8	3.4	4.6	3.2	15.1	4	3.3	4.1	2	8.8	1.2	9.7	4.6	2.2	4	1.6	0.9	3.2	2.8	3.4	0.8	1.7	1.2	1.2	5.3	0.7	3.7
Ta	0.7	0.9	0.1	0.8	0.3	0.3	2	0.9	0.5	1	0.4	1.6	0.3	1.5	1.7	0.5	0.9	0.2	0.1	0.9	0.7	1.1	0.2	0.4	0.28	0.26	0.9	0.22	0.62

JSR A
Journal of Scientific Reports

Karadirek, S., Journal of Scientific Reports-A, Number 52, 65-98, March 2023.

W	2.2	2.8	1.4	3.6	2.3	1.7	3.7	7.8	1.5	2.7	1.9	7.2	0.6	4.1	2.9	4.3	1.8	0.7	1.8	2.6	2.6	3.6	1.3	1.3	1.1	1.2	1.9	1	1.1
Hg	0.16	0.13	0.07	0.05	0.1	0.29	0.16	0.11	0.19	0.31	0.5	0.15	0.28	0.11	0.23	0.16	0.2	0.17	0.12	0.11	0.15	0.33	0.06	0.04	0.1	0.1	0.05	0.17	0.16
Pb	29.3	31	4.6	22.5	7.9	19	120.3	20.9	19.8	19.2	30.1	78.2	7.7	82.5	23	9.4	20	8	4.1	28.7	30.3	30.2	5.3	15.7	7.8	6.6	17	11	15.1
Bi	0.4	0.4	0.1	0.4	0.3	0.1	1.2	0.4	0.2	0.4	0.5	1	0.1	0.9	0.5	0.1	0.4	0.1	0.1	0.3	0.3	0.2	0.1	0.1	0.97	0.84	0.16	<1	0.79
Th	13.7	18.9	3.3	23.7	13.1	7.1	100.6	22.6	16.6	24.3	18.7	73	7.1	66.1	26.6	7.4	23.7	6.2	2.9	14.2	12.7	9.3	3.4	6.3	3.3	3.3	10.5	3.2	5.8
U	2.6	7.9	1.4	7	5.9	2.1	29	6.4	3.9	4.5	4.1	21.8	0.8	20.7	5.5	3.9	6.1	1.7	0.4	2.9	2.4	2.1	1.6	1.5	2.4	2.9	2.7	2.1	2.4
V/Ni	0.08	0.11	0.08	0.26	0.36	0.09	0.73	0.21	0.08	0.06	0.04	0.49	0.06	0.28	0.05	0.12	0.05	0.08	0.07	0.14	0.08	0.08	0.12	0.15	-	-	-	-	-
V/(V+Ni)	0.07	0.10	0.08	0.21	0.26	0.08	0.42	0.18	0.07	0.06	0.04	0.33	0.06	0.22	0.04	0.11	0.05	0.08	0.07	0.12	0.08	0.08	0.11	0.13	-	-	-	-	-
Sr/Cu	1.38	1.50	2.96	2.93	3.93	4.10	86.72	1.92	1.90	1.53	1.99	19.17	3.72	24.45	1.99	2.20	1.82	0.62	2.18	4.58	3.12	3.37	1.95	4.59	-	-	-	-	-
Ga/Rb	0.20	0.20	0.22	0.23	0.28	0.33	1.02	0.18	0.13	0.18	0.17	0.41	0.22	0.54	0.18	0.29	0.16	0.22	0.25	0.17	0.17	0.22	0.21	0.18	-	-	-	-	-
U/Th	0.19	0.42	0.42	0.30	0.45	0.30	0.29	0.28	0.23	0.19	0.22	0.30	0.11	0.31	0.21	0.53	0.26	0.27	0.14	0.20	0.19	0.23	0.47	0.24	-	-	-	-	-

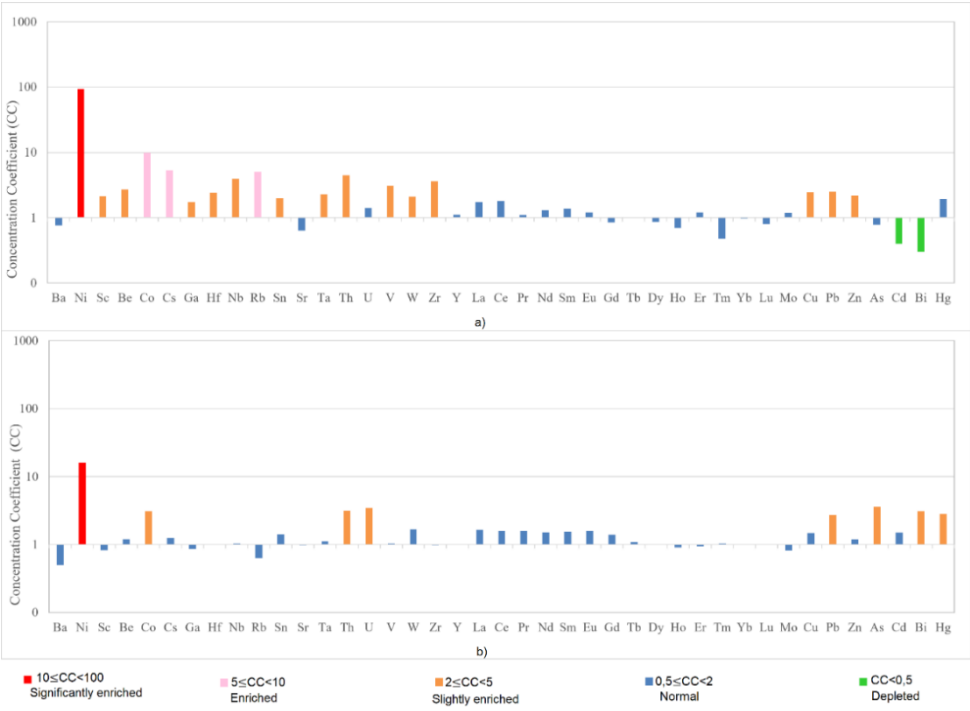

Figure 7. Concentration coefficients of trace elements of studied samples a) coal, b) parting, roof, and floor.

Several elements (e.g. S, B, U, Ba, Ni) and their ratios (e.g. Th/U, V/(V+Ni), Ni/Co, Sr/Cu) can be used as indicators (salinity, paleoredox conditions and paleoclimate) for the depositional environment during or after peat deposition. Especially when evaluating the formation environment of coal, the water chemistry of the sedimentation environment and the elemental chemistry of the coal may differ due to various effects in diagenetic or epigenetic processes. Therefore, elements with similar geochemical behavior or related element ratios should be used rather than a single element [81]. V/Ni, V/(V+Ni), which are redox sensitive geochemical indices, are widely used in sedimentary rocks rather than other trace element ratios [2, 82, 83]. A high V/Ni (>3) reducing environment indicates a V/Ni suboxic environment between 1.9-3, whereas a low (<1.9) V/Ni ratio indicates oxic environments [84]. Moreover, high (>1) V/Ni ratios indicate marine carbonates or siliciclastics, while low (<1) values indicate lacustrine or terrestrial origin [85]. ((El-Sabagh et al., 2018). V/(V +Ni) ratios ≤0.46, 0.46-0.60, 0.54-0.82 and >0.84 indicate oxic, dysoxic, suboxic-anoxic and euxinic environments, respectively [86].. Low V/Ni and V/(V + Ni) ratios in the studied samples indicate oxidizing conditions and lacustrine origin (Table 4) and are consistent with the sedimentation environment of coal. U/Th ratios are other redox sensitive ratios used to determine the depositional environment of organic matter-rich deposits [87]. U/Th ratio <0.75 indicates oxic, 0.75-1.25 indicates suboxic, >1.25 indicates suboxic-anoxic depositional environment [82]. Tunçbilek-Tavşanlı coal samples of roof,

parting and floor presented low (<0.84) values. Other ratios that provide information about the precipitation environment by using element ratios are Sr/Cu and Ga/Rb ratios. In particular, the Sr/Cu and Ga/Rb ratios of fine-grained sediments provide information about the climatic changes of the deposition environment. Sr/Cu ratios between 1.3–5.0 are associated with humidity, while values greater than 5.0 are associated with drought [88]. Ga/Rb ratios offer lower values as the temperature decreases [89]. Parting samples taken from the Tunçbilek-Tavşanlı field indicate arid climate, while other samples vary and indicate a humid climate.

4.2.3. Rare earth elements and yttrium (REE+Y or REY)

The total REE+Y concentration in the studied samples of Tunçbilek-Tavşanlı coal seam ranges between 25.77 and 167.26 µg/g (Table 5), with an average of 95.04 µg/g, which is higher than the average REE+Y concentration of world's low-rank coals (65.27 µg/g; [75]). This average value corresponds to 0.7 times the average REE+Y concentration (135.89 µg/g; [91, 3, 6]) of Chinese coals, and corresponds to 1.5 times the average REE+Y concentration (62.09 µg/g; [90]) of USA coals. REE+Y concentrations were normalized to UCC values to show the REE+Y distribution patterns of the studied samples (Fig. 8).

Correlation coefficient between ash content and REE+Y concentrations is high (r=0.74; Table 3). The coal sample with the highest ash content (TFC17) has the maximum REE+Y concentration (152.4 µg/g) and the minimum REE+Y value (25.8 µg/g) is the coal sample with the lowest ash content (TFC19; 8.2 µg/g), which is an indication of mineral matter association for REE+Y in Tunçbilek-Tavşanlı coal samples. It has been stated that REYs in low rank coals in Turkey are generally associated with tuff type, acid and alkaline volcanic ash and formed in the peat bog stage [92]

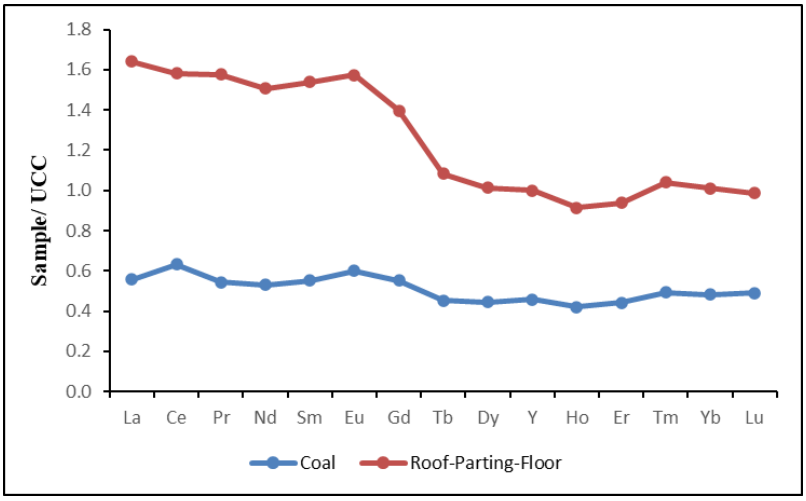

Figure 8. REE+Y distribution patterns of FC pano samples of Tunçbilek-Tavşanlı basin.

As suggested by Seredin and Dai (2012) [13], three enrichment phases of rare earth elements and yttrium in coal are adopted in this study:

1) "Light REE (La, Ce, Pr, Nd and Sm) enrichment (L-type; $La_N/Lu_N > 1$); $_N$: REE+Y concentrations in the studied samples normalized by average values of UCC [93]";
2) "Medium REE+Y (Eu, Gd, Tb, Dy and Y) enrichment (M-type; $La_N/Sm_N < 1$, $Gd_N/ Lu_N > 1$)";
3) "Heavy REE (Ho, Er, Tm, Yb and Lu) enrichment (H-type; $La_N/Lu_N < 1$)."

Table 5. REE+Y contents of studied samples of Tunçbilek -Tavşanlı coalfield.

Sample	La	Ce	Pr	Nd	Sm	Eu	Gd	Tb	Dy	Y	Ho	Er	Tm	Yb	Lu	REE+Y
TFC1	23.7	46.9	5.05	18.5	3.53	0.83	3.26	0.47	2.46	14.4	0.51	1.50	0.21	1.46	0.23	123.0
TFC2	30.2	67.9	6.90	26.1	4.85	1.17	4.40	0.62	3.32	17.1	0.66	1.83	0.27	1.68	0.26	167.3
TFC3	6.6	10.7	1.05	4.0	0.63	0.21	0.61	0.10	0.54	3.3	0.13	0.34	0.05	0.32	0.06	28.6
TFC4	22.3	51.8	5.43	20.2	3.43	0.80	2.76	0.39	2.16	12.1	0.41	1.18	0.17	1.13	0.17	124.4
TFC5	19.0	41.1	4.48	16.5	2.96	0.65	2.46	0.41	2.38	14.6	0.50	1.43	0.21	1.38	0.23	108.3
TFC6	12.9	24.9	2.77	10.0	1.94	0.42	1.58	0.24	1.42	10.6	0.34	1.04	0.16	1.18	0.22	69.7
TFC7	146.1	282.4	31.92	114.0	19.17	3.79	13.78	1.68	8.38	43.9	1.49	4.30	0.63	4.04	0.59	676.2
TFC8	23.6	59.4	5.37	20.6	3.79	0.86	3.11	0.43	2.50	12.8	0.47	1.50	0.22	1.48	0.22	136.4
TFC9	17.2	43.3	3.89	14.6	2.54	0.55	1.94	0.27	1.34	6.5	0.27	0.74	0.11	0.73	0.11	94.1
TFC10	22.8	49.6	5.09	18.9	3.30	0.81	2.89	0.42	2.19	11.7	0.45	1.33	0.19	1.19	0.19	121.1
TFC11	17.8	45.9	3.93	13.9	2.52	0.55	2.02	0.28	1.48	8.3	0.29	0.83	0.13	0.86	0.13	98.9
TFC12	91.2	185.0	21.06	75.3	13.13	2.75	8.83	1.14	5.58	26.0	0.96	2.60	0.38	2.35	0.34	436.6
TFC13	7.3	17.4	1.79	7.0	1.45	0.32	1.21	0.18	0.95	5.4	0.19	0.61	0.09	0.51	0.08	44.5
TFC14	91.9	175.7	20.26	73.8	12.63	2.77	9.00	1.20	6.27	33.0	1.16	3.21	0.47	2.97	0.46	434.8
TFC15	26.8	64.9	6.30	23.0	4.36	1.00	3.93	0.55	3.09	17.4	0.60	1.74	0.25	1.55	0.25	151.7
TFC16	6.9	15.6	1.42	4.8	0.94	0.23	0.81	0.13	0.74	4.2	0.13	0.42	0.06	0.41	0.06	36.9
TFC17	27.9	67.8	6.10	22.5	4.00	0.93	3.47	0.47	2.51	13.0	0.52	1.46	0.20	1.32	0.19	152.4
TFC18	11.8	27.4	2.64	9.7	1.60	0.37	1.35	0.18	0.90	4.5	0.18	0.50	0.07	0.44	0.06	61.7
TFC19	6.2	9.9	0.91	3.4	0.62	0.15	0.54	0.09	0.53	2.6	0.10	0.31	0.04	0.33	0.05	25.8
TFC20	29.9	57.2	6.47	23.3	4.58	1.04	3.88	0.58	3.20	17.5	0.68	2.00	0.29	1.88	0.28	152.8
TFC21	26.4	49.8	5.35	19.9	3.67	0.82	3.08	0.45	2.41	13.5	0.51	1.60	0.23	1.61	0.26	129.6
TFC23	21.6	49.6	5.36	21.8	4.56	1.18	4.77	0.73	4.12	21.2	0.83	2.27	0.33	2.12	0.32	140.8

TFC24	7.0	13.7	1.41	5.7	1.07	0.29	0.98	0.15	0.80	5.3	0.19	0.54	0.08	0.50	0.07	37.8
TFC25	19.8	36.1	3.88	13.7	2.71	0.69	2.71	0.42	2.33	14.1	0.49	1.41	0.19	1.28	0.20	100.0
World [75]	11	23	4.0	12	2.00	0.47	2.70	0.32	2.10	8.4	0.54	0.93	0.31	1.00	0.20	68.97
Lignite [75]	10	22	3.5	11	1.90	0.50	2.60	0.32	2.00	8.6	0.50	0.85	0.31	1.00	0.19	65.27
UCC [80]	31	63	7.1	27	4.70	1.00	4.00	0.70	3.90	21.0	0.83	2.30	0.30	2.00	0.31	169.14
USA [81]	12	21	2.4	9.5	1.70	0.40	1.80	0.30	1.90	8.5	0.35	1.00	0.15	0.95	0.14	62.09
China[3,6,82]	22.5	46.7	6.42	22.3	4.07	0.84	4.65	0.62	3.74	18.2	0.96	1.79	0.64	2.08	0.38	135.89

Coal is characterized by an L-type enrichment, except for TFC5, TFC6 samples with H-type enrichment and TFC12, TFC23, TFC24 samples with M-L type enrichment in the roof, floor, and parting samples, respectively (Table 6).

Since Ce, Eu and Gd anomalies occur only under certain geochemical conditions, they can be used as indicators to reflect the paleoenvironmental characteristic sediment-source region, and tectonic evolution [94]. However, Eu is inhibited by Ba concentrations in many cases, as stated by Dai et al. (2016) [94] and Yan et al. (2018, 2019) [95, 96]. The positive correlation between Ba and Eu concentrations in coal (Fig. 9a) and the Ba/Eu ratio, which ranged from 37.8 to 434.4 and averaged 148.6 in coal samples, was found by Yan et al. (2018) [95]. It clearly shows Ba interference on Eu, although it is lower than the interference threshold Ba/Eu=1000. Again, the weak correlation between Ba and Eu concentrations in non-coal samples (Fig. 9b) indicates that Ba do not interact with Eu in these samples despite low Ba/Eu ratios (ranging from 116 to 339). Therefore, no interpretation could be made for the samples.

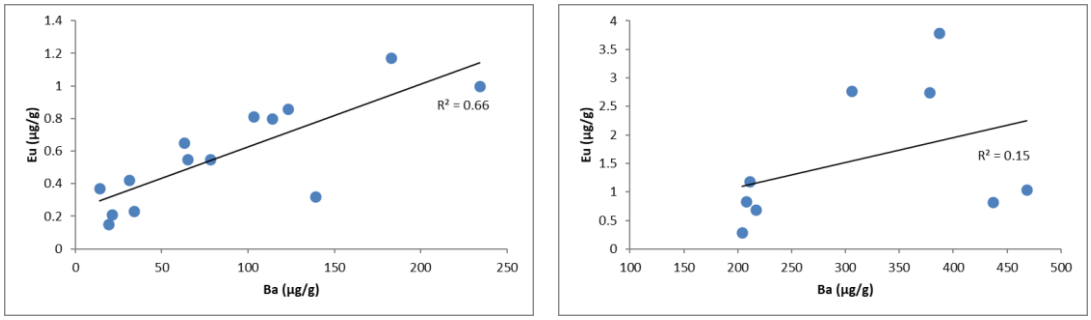

Figure 9. Relationship between Ba and Eu concentrations of studied samples a) coal samples; b) roof, floor, and parting.

Furthermore, redox-sensitive Ce and Eu anomalies (in non-coal samples) and in some cases, non-redox-sensitive La, Gd, and Y anomalies in coal may change under certain geochemical conditions [94]. In this study, the Eq. 1-3 were used to measure the separation of Ce, Eu and Gd concentrations from other REE+Y in dispersion models.

$$Eu_N/Eu_N^{*} = Eu_N /[(Sm_N \times 0.67) + (Tb_N \times 0.33)] \quad (1)$$

$$Ce_N/Ce_N^{*} = Ce_N/[(La_N \times 0.5) + (Pr_N \times 0.5)] \quad (2)$$

$$Gd_N/Gd_N^{*} = Gd_N/[(Sm_N \times 0.33) + (Tb_N \times 0.67)] \quad (3)$$

Respectively, in the calculations of Gd_N/Gd_N^{*} and Eu_N/Eu_N^{*}, Tb is used instead of Eu to avoid confusion of Eu anomaly with Gd anomaly and in order to avoid confusion of the Gd anomaly with the Eu anomaly, Tb is used instead of Gd concentration. The Y_N/Ho_N ratio in coal is used to represent the divergence of geochemical twins Y and Ho, which produces Y anomalies in the REE+Y

JSR A
Journal of Scientific Reports

Karadirek, S., Journal of Scientific Reports-A, Number 52, 65-98, March 2023.

classification. Values Y_N/Ho_N <1 and >1 represent negative and positive anomalies, respectively [94]. While Ce in the studied coal samples generally shows weak positive anomaly; Ce in the non-coal samples is generally characterized by negative anomaly (Table 6). Generally, groundwater or hydrothermal leak of roof, parting and floor can cause Ce anomalies in both coals and non-coal fractions. During non-coal leaching, Ce^{3+} can be converted to Ce^{4+}, which is preferentially precipitated in-situ[97]. Thus, non-coal fractions show Ce-depletion relative to coals, but cause leaks richer in REY, and it usually indicates oxidizing conditions for the leaching process [2]. In the studied samples, the REY values are higher, while the Ce anomaly in the roof and floor samples is lower than the coals. Eu element, another redox sensitive rare earth element, is not recommended to be used in coals[65]. Eu and Gd show weak positive anomalies in all samples (Table 6). Yttrium shows positive anomaly in coal samples except TFC7, TFC17 and TFC18 and in non-coal samples. If peat interacts with sea water, it generally shows positive anomalies for La, Gd and Y[98]. However, since coals are also affected by hydrothermal fluids during peat deposition, positive anomalies for La, Gd and Y may be under the combined influence of seawater and hydrothermal fluids [76]. Since the study area exhibits lacustrine environment characteristics, positive anomalies of La, Gd and Y can be attributed to hydrothermal fluids.

Table 6. Anomalies and enrichment patterns of Eu, Ce, Gd and Y of coal samples in Tunçbilek-Tavşanlı coal basin.

Sample	Eu_N/Eu_{N*}	Ce_N/Ce_{N*}	Gd_N/Gd_{N*}	La_N/Lu_N	La_N/Sm_N	Gd_N/Lu_N	Y_N/Ho_N	ET	C_{outl}	Critic REE+Y	Non-critic REE+Y	Super Critic REE+Y
TFC1	1.15	1.01	1.17	1.03	1.02	1.10	1.12	L	0.77	38.16	35.54	49.31
TFC2	1.19	1.11	1.18	1.16	0.94	1.31	1.02	L-M	0.71	50.14	46.35	70.77
TFC3	1.53	0.94	1.09	1.10	1.59	0.79	1.00	L	0.75	8.49	8.89	11.26
TFC4	1.19	1.11	1.12	1.31	0.99	1.26	1.17	L-M	0.69	36.83	33.92	53.68
TFC5	1.06	1.05	1.02	0.83	0.97	0.83	1.15	H	0.83	35.97	28.90	43.42
TFC6	1.08	0.98	1.08	0.59	1.01	0.56	1.23	H	0.89	23.72	19.19	26.80
TFC7	1.08	0.97	1.17	2.48	1.16	1.81	1.16	L	0.61	176.05	210.97	289.15
TFC8	1.16	1.24	1.15	1.07	0.94	1.10	1.08	L-M	0.63	38.69	35.87	61.79
TFC9	1.12	1.25	1.11	1.56	1.03	1.37	0.95	L	0.54	24.00	25.57	44.52
TFC10	1.21	1.08	1.14	1.20	1.05	1.18	1.03	L	0.68	35.35	34.08	51.62
TFC11	1.12	1.29	1.13	1.37	1.07	1.20	1.13	L	0.54	25.34	26.27	47.31
TFC12	1.14	0.99	1.10	2.68	1.05	2.01	1.07	L-M	0.60	113.37	134.22	189.03
TFC13	1.10	1.13	1.10	0.91	0.76	1.17	1.12	M	0.79	14.46	11.75	18.27
TFC14	1.17	0.96	1.11	2.00	1.10	1.52	1.12	L	0.67	120.25	133.79	180.76
TFC15	1.14	1.18	1.18	1.07	0.93	1.22	1.15	M	0.69	46.78	41.39	67.55
TFC16	1.18	1.17	1.06	1.15	1.11	1.05	1.28	L	0.65	10.52	10.07	16.26
TFC17	1.17	1.22	1.19	1.47	1.06	1.42	0.99	L	0.58	40.87	41.47	67.55
TFC18	1.18	1.16	1.19	1.97	1.12	1.74	0.99	L	0.57	16.15	17.39	28.15
TFC19	1.15	0.96	1.04	1.24	1.52	0.84	1.03	L	0.68	7.08	8.27	10.42

TFC20	1.12	0.97	1.11	1.07	1.00	1.07	1.02	L	0.79	47.62	44.83	60.33
TFC21	1.12	0.98	1.12	1.02	1.09	0.92	1.05	L	0.74	38.68	38.50	52.41
TFC23	1.19	1.08	1.17	0.68	0.72	1.16	1.01	M-H	0.96	51.30	36.29	53.20
TFC24	1.30	1.02	1.12	1.00	0.99	1.09	1.10	L-M	0.88	12.78	10.46	14.54
TFC25	1.18	0.97	1.14	0.99	1.11	1.05	1.14	L	0.85	32.65	29.10	38.26

Seredin and Dai (2012) [13] developed a new classification for the evaluation of REE+Y in coal as an economic raw material, which considers REE+Y degree, element composition, resources of rare metals, exploitable tonnage of coal, formation forms of rare metals in coal and coal burning production, extraction methods, environmental problems, supply and demand relationship of rare metals [65]. According to this classification, REE+Y is divided into three groups namely critical (Nd, Eu, Tb, Dy, Y and Er), non-critical (La, Pr, Sm ve Gd) and super critical (Ce, Ho, Tm, Yb and Lu). In the studied samples, the critical and non-critical groups present close values in the total REE+Y concentration, while the REE+Y concentration of the super critical groups constitutes a significant portion of the total REE+Y concentration in the coal, roof, floor and parting samples (Table 6).

Dai et al. (2017) [65] stated that REE+Y content greater than 1000 µg/g is considered as the cut-off grade for useful recovery, and the second criterion is $REE+Y_{def}$, rel-C_{outl} graph. Where $REE+Y_{def}$ stands for the percentage of critical elements in total REE+Y, C_{outl} (outlook coefficient) is the ratio of relative amount of critical REE+Y metal in the total REE+Y. Excessive REE+Y is calculated by Eq. 4:

$$Coutl= (Nd + Eu + Tb + Dy + Er + Y / \Sigma REE+Y)/(Ce + Ho + Tm + Yb + Lu / \Sigma REE+Y) \quad (4)$$

REE+Y sources with $0.7 \leq C_{outl} \leq 1.9$ and $C_{outl} > 2.4$ are considered as promising and highly promising, respectively [65]. The C_{outl} values of Tunçbilek-Tavşanlı samples were calculated and given in Table 6. According to the relationship between the cut-off grade and C_{outl}, the coal, roof, floor and parting layers remain within the unpromising area (Fig. 10).

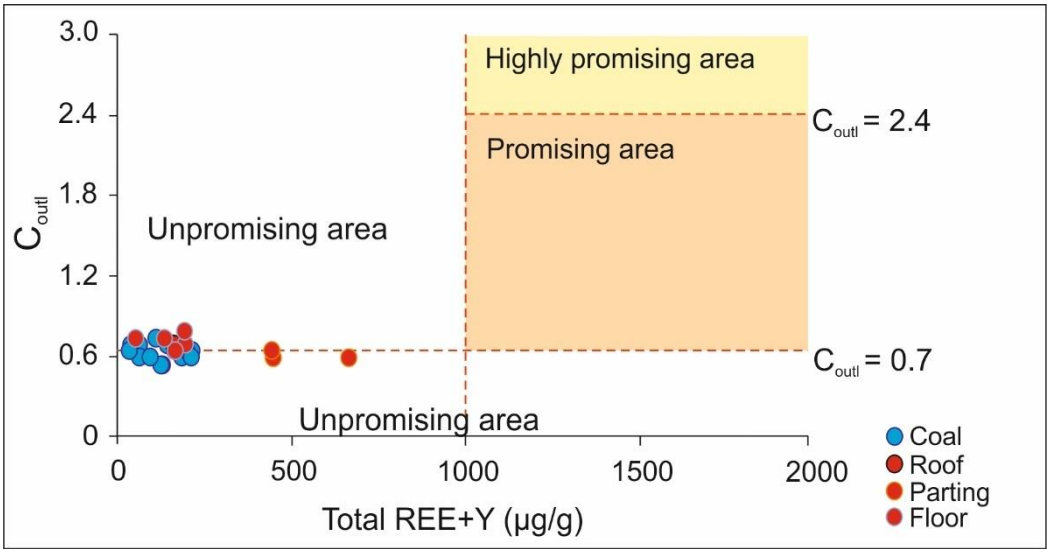

Figure 10. Evaluation of REE+Y in coal and host rock samples of Tunçbilek-Tavşanlı coal field [65].

5. CONCLUSION

The minerals in the studied coal samples are, in order of abundance, quartz, kaolinite, illite-smectite and siderite, dolomite, illite, smectite, mica, feldspar, pyrite, chlorite and jarosite. The mineral compositions of the samples taken from the roof-floor-parting showed similarities with the coal samples. SiO_2, Al_2O_3 and Fe_2O_3 are generally the most abundant major oxides in the studied samples. The MgO, K_2O, CaO, TiO_2, Na_2O, P_2O_5 and MnO were also detected in lesser amounts. Only in the parting samples, SiO_2, Al_2O_3 and MgO are the most abundant major oxides whereas Fe_2O_3, K_2O, TiO_2, CaO, P_2O_5, Na_2O and MnO were found to be in lesser amounts. It was observed that the major oxide contents were high in claystone and carbonaceous shale samples. Concentration of SiO_2 and Al_2O_3 in coal samples is quite low comparing to other samples and the main source of SiO_2 and Al_2O_3 is kaolinite and illite-smectite mixed-layer clays. Samples with high Al_2O_3 content are abundant in kaolinite, however, SiO_2 may be partially related to the quartz content. Siderite and pyrite minerals are relatively abundant in samples with high Fe_2O_3. It was observed that dolomite minerals were more abundant in samples with high MgO.

The CC values of Tunçbilek-Tavşanlı coals are predominantly in the slightly enriched-normal ranges, whereas the CC values of the roof, floor and parting samples present normal values. According to the concentration coefficient, the Ni element in the coals is significantly enriched; Cs, Co and Rb elements are enriched and are of inorganic origin. REE+Y concentration (average 95.04 µg/g) is higher than the average REE+Y concentration of world's low-rank coals and USA coals. In samples with high ash content, REE+Y concentration is high, while relatively low concentration of REE+Y in samples with low ash content indicates mineral matter relationship. This shows that it may be related to the tuffy units in the coal basin. The Eu, Ce, Gd and Y values of coal seam samples of Tunçbilek

Formation show weak positive anomalies. This suggested that it may be related to hydrothermal fluids. Based on the Al_2O_3/TiO_2 ratio and the L-type enrichment of REE+Y, it can be concluded that the terrestrial materials around the coal basin in the early stage of peat deposition are mainly derived from intermediate-felsic tuffs. Element ratios (V/Ni, V/(V +Ni), U/Th) indicate oxidizing conditions and lacustrine origin. In addition, the Sr/Cu and Ga/Rb ratios of the roof, coal and floor strata samples indicate humid conditions, whereas the Sr/Cu and Ga/Rb ratios of parting strata samples indicate relatively arid climate. The usability of REE+Y in Tunçbilek-Tavşanlı coals as an industrial raw material source does not constitute a potential source according to the cut-off grade-C_{outl} association, although the extremely critical groups (Ce, Ho, Tm, Yb and Lu) are dominant.

ACKNOWLEDGEMENT

This study was funded by Akdeniz University Research Coordination Unit (FYL-2019-5015). The author would like to thank Turkish Coal Enterprises for their support during field work and sampling, and all the reviewers for their valuable comments and contributions.

REFERENCES

[1] Thurber, M.C., Morse, R.K., (2015), The Global Coal Market: Supplying Major Fuel for Emerging Economies, Cambridge University Press, Cambridge, 702 p.

[2] Dai, S., Bechtel, A., Eble, C.F., Flores, R.M., French, D., Graham, I.T., Hood, M.M., Hower, J.C., Korasidis, V.A., Moore, T.A., Puttmann, W., Wei, Q., Zhao, L., O'Keefem, J.M.K., (2020), Recognition of peat depositional environments in coal: A review, International Journal of Coal Geology, 219, 103383.

[3] Dai, S., Tian, L., Chou, C.L., Zhou, Y., Zhang, M., Zhao, L., Wang, J., Yang, Z., Cao, H., Ren, D., (2008a), Mineralogical and compositional characteristics of Late Permian coals from an area of high lung cancer rate in Xuan Wei, Yunnan, China: occurrence and origin of quartz and chamosite, International Journal of Coal Geology, 76, 318–327.

[4] Dai, S., Ren, D., Zhou, Y., Chou, C.L., Wang, X., Zhao, L., Zhu, X., (2008b), Mineralogy and geochemistry of a superhigh-organic-sulfur coal, Yanshan Coalfield, Yunnan, China: evidence for a volcanic ash component and influence by submarine exhalation, Chemical Geology, 255, 182–194.

[5] Dai, S., Wang, X., Chen, W., Li, D., Chou, C.L., Zhou, Y., Zhu, C., Li, H., Zhu, X., Xing, Y., Zhang, W., Zou, J., (2010), A high-pyrite semianthracite of Late Permian age in the Songzao Coalfield, southwestern China: mineralogical and geochemical relations with underlying mafic tuffs, International Journal of Coal Geology, 83, 430–445.

[6] Dai, S., Ren, D., Chou, C.L., Finkelman, R.B., Seredin, V.V., Zhou, Y., (2012), Geochemistry of trace elements in Chinese coals: a review of abundances, genetic types, impacts on human health, and industrial utilization, International Journal of Coal Geology, 94, 3-21.

[7] Finkelman, R.B., Dai, S., French, D., (2019), The importance of minerals in coal as the hosts of chemical elements, International Journal of Coal Geology, 212, 103251.

[8] Dai, S., Finkelman, R.B., (2018), Coal as a promising source of critical elements: progress and future prospects, International Journal of Coal Geology, 186, 155–164.

[9] Güllüdağ, C.B., Aksoy, E., Ünal, N., Özmen, S.F., (2020), Radioactivity concentrations and risk assessment of Tekirdağ lignites (case study of Malkara coalfield), Acta Geophysica, 68, 1411–1420.

[10] Seredin, V.V., Finkelman, R.B., (2008), Metalliferous coals: A review of the main genetic and geochemical types, International Journal of Coal Geology, 76, 253–289.

[11] Lin, R., Soong, Y., Granite, E.J., (2018b), Evaluation of trace elements in U.S. coals using the USGS COALQUAL database version 3.0. Part II: Non-REY critical elements, International Journal of Coal Geology, 192, 39–50.

[12] Zhao, L., Ward, C.R., French, D., Graham, I.T., Dai, S., Yang, C., Xie, P., Zhang, S., (2018), Origin of a kaolinite-NH_4-illite-pyrophyllite-chlorite assemblage in a marine-influenced anthracite and associated strata from the Jincheng Coalfield, Qinshui Basin, Northern China, International Journal of Coal Geology, 185, 61–78.

[13] Seredin, V.V., Dai, S., (2012), Coal deposits as potential alternative sources for lanthanides and yttrium, International Journal of Coal Geology, 94, 67–93.

[14] Hower, J.C., Eble, C.F., Dai, S.F., Belkin, H.E., (2016), Distribution of rare earth elements in eastern Kentucky coals: indicators of multiple modes of enrichment?, International Journal of Coal Geology, 160, 73–81.

[15] Kolker, A., Scott, C., Hower, J.C., Vazquez, J.A., Lopano, C.L., Dai, S., (2017), Distribution of rare earth elements in coal combustion fly ash, determined by SHRIMP-RG ion microprobe, International Journal of Coal Geology, 184, 1–10.

[16] Laudal, D.A., Benson, S.A., Addleman, R.S., Palo, D., (2018), Leaching behavior of rare earth elements in Fort Union lignite coals of North America, International Journal of Coal Geology, 191, 112–124.

[17] Lin, R., Soong, Y., Granite, E.J., (2018a), Evaluation of trace elements in U.S. coals using the USGS COALQUAL database version 3.0. Part I: rare earth elements and yttrium (REY), International Journal of Coal Geology, 192, 1–13.

[18] Wagner, N.J., Matiane, A., (2018), Rare earth elements in select Main Karoo Basin (South Africa) coal and coal ash samples, International Journal of Coal Geology, 196, 82–92.

[19] Seredin, V.V., (2012), From coal science to metal production and environmental protection: a new story of success, International Journal of Coal Geology, 90, 1–3.

[20] Dai, S., Yan, X., Ward, C.R., Hower, J.C., Zhao, L., Wang, X., Zhao, L., Ren, D., Finkelman, R.B., (2018), Valuable elements in Chinese coals: a review, International Geology Review, 60, 590–620.

[21] Arni, P., (1942), Anadolu ofiyolitlerinin yaşlarına mütedir malumat, Bulletin of the Mineral Research and Exploration, 28, 472-488.

[22] Nebert, K., (1960), Tavşanlı'nın batı ve kuzeyindeki linyit ihtiva eden Neojen sahasının mukayeseli stratigrafisi ve tektoniği, Bulletin of the Mineral Research and Exploration, 54, 7-35.

[23] Kalafatçıoğlu, A., (1962), A note on the geology of the region between Tavşanlı and Dağardı, and on the age of the serpentines and limestones, Bulletin of the Mineral Research and Exploration, 58, 38-46.

[24] Okay, A.I., (1981), The geology and blueschist metamorphism of the ophiolites in Northwest Turkey (Tavşanlı-Kütahya), Bulletin of the Geological Society of Turkey, 24, 85-95.

[25] Okay, A.I., (1984), Kuzeybatı Anadolu'da yer alan metamorfik kuşaklar, Ketin Sempozyumu, pp. 83-92.

[26] Baş, H., (1986), Tertiary geology of the Domaniç-Tavşanlı-Kütahya-Gediz region, Geological Engineering, 11-18.

[27] Helvacı, C., İnci, U., Yağmurlu, F., Yılmaz, H., (1987), Neogen stratigraphic and economic potential of Western Turkey, Journal of Isparta Engineering Faculty of Akdeniz University, 3, 31-45.

[28] Kocyigit, A., Bozkurt, E., (1997), Kütahya-Tavşanlı çöküntü alanının neotektonik özellikleri, TÜBİTAK Project No: YDABÇAG-126, 78 p.

[29] Günal Türkmenoğlu, A., Yavuz-Işık, N., (2007), Mineralogy, chemistry and potential utilization of clays from coal deposits in the Kütahya province, Western Turkey, Applied Clay Science, 42, 63-73.

[30] Özburan, M., (2009), Neotectonic investigation of Kütahya and Its surrounding, Dissertation, Kocaeli University, 209 p.

[31] Göncüoğlu, M.C., (2011), Geology of the Kütahya-Bolkardağ belt, Bulletin of the Mineral Research and Exploration, 142, 223-277.

[32] Erkoyun, H., Kadir, S., Huggett, J., (2019), Occurrence and genesis of tonsteins in the Miocene lignite, Tunçbilek Basin, Kütahya, western Turkey, International Journal of Coal Geology, 202, 46-68.

[33] Soytürk, T., (1992), Tunçbilek kömürlerinin kendiliğinden yanmaya yatkınlıklarının araştırılması, Dissertation, Anadolu University, 76 p.

[34] Yavuz, N., (1994). Palynology, petrography and chemistry of the Tavşanlı coals (Kütahya), Dissertation, Middle East Technical University, Ankara, , 90 p.

[35] Bacak, G., (2003). Mineralogical, petrographical and petrogenetical study of Southern Dağardı (Tavşanlı-Kütahya) ophiolite, Dissertation, İstanbul Technical University, İstanbul, 284 p.

[36] Karayigit, A.I., Celik, Y., (2003), Mineral matter and trace elements in Miocene coals of the Tuncbilek-Domanic Basin, Kutahya, Turkey, Energy Sources, 25, 339-355.

[37] Parlak, A., (2010), Briquetting Tunçbilek lignites and retention of sulfur in ash during combustion, Dissertation, Gazi University, Ankara, 104 p.

[38] Akkiraz, M.S., Akgün, F., Utescher, T., Wilde, V., Bruch, A.A., Mosbrugger, V., Üçbaş, S.D., (2012), Palaeoflora and climate of lignite-bearing lower–middle Miocene sediments in the Seyitömer and Tunçbilek sub-basins, Kütahya province, Northwest Turkey, Turkish Journal of Earth Sciences, 21, 213-235.

[39] Helvacı, C., Ersoy, E.Y., Billor, M.Z., (2017), Stratigraphy and Ar/Ar geochronology of the Miocene lignite‐bearing Tunçbilek‐Domaniç Basin, western Anatolia, Inernational Journal of Earth Science, 106, 1797-1814.

[40] Akçay, A., (2017), Neotectonic investigation of the coaly Neogene area between Kızılbük-Degirmisaz (Tavşanlı/Kütahya), Dissertation, Dumlupınar University, 67 p.

[41] Emre, Ö., Duman, T.Y., Özalp, S., Şaroğlu, F., Olgun, Ş., Elmacı, H., Çan, T., (2018), Active fault database of Turkey, Bulletin of Earthquake Engineering, 16, 3229-3275.

[42] Akgün, E., Özden, S., (2019), Plio-Quaternary stress states along the Kütahya Fault and surroundings, NW Turkey, Turkish Journal of Earth Sciences, 28, 671-686.

[43] Kezer, Z., (2019), Tectonic geomorphology of the Kütahya Graben (Western Anatolia), Dissertation, Hacettepe University, 92 p.

[44] Kazancı, C., (2019), Organic facies characteristics of FC pano opencast mine coals, Tunçbilek (Tavşanlı-Kütahya), Dissertation, Akdeniz University, Antalya, 67 p.

[45] Cicioglu Sutcu, E., Şentürk, S., Kapıcı, K., Gökçe, N., (2021), Mineral and rare earth element distribution in the Tunçbilek coal seam, Kütahya, Turkey, International Journal of Coal Geology, 245, 103820.

[46] Ketin, İ., (1966), Tectonic Units of Anatolia, Bulletin of the Mineral Research and Exploration, 66, 20-37.

[47] Okay, A.I., Tüysüz, O., (1999), Tethyan sutures of northern Turkey, Geological Society Special Publication, 156 (1), 475−515.

[48] Şengör, A.M.C., Yılmaz, Y., (1981), Tethyan evolution of Turkey: a plate tectonic approach, Tectonophysics, 75, 181-241.

[49] Candan, O., Koralay, O.E., Akal, C., Kaya, O., Oberhänsli, R., Dora, O.Ö., Konak, N., Chen, F., (2011), Supra-Pan-African unconformity between core and cover series of the Menderes Massif/Turkey and its geological implications, Precambrian Research, 184, 1–23.

[50] Candan, O., Çetinkaplan, M., Oberhänsli, R., Rimmelé, G., Akal, C., (2005), Alpine high-P/low-T metamorphism of the Afyon Zone and implications for the metamorphic evolution of Western Anatolia, Turkey, Lithos, 84, 102-124.

[51] Göncüoğlu, M.C., Sayit, K., Tekin, U.K., (2010), Oceanization of the northern Neotethys: geochemical evidence from ophiolitic melange mélange basalts within the İzmir-Ankara suture belt, NW Turkey, Lithos, 116, 175–187.

[52] Okay, A.I., Harris, N.B.W., Kelley, S.P. (1998), Exhumation of blueschists along a Tethyan suture in northwest Turkey, Tectonophysics, 285, 275–299.

[53] Okay, A.I., Tansel, I., Tüysüz, O., (2001), Obduction, subduction and collision as reflected in the Upper Cretaceous–Lower Eocene sedimentary record of Western Turkey, Geological Magazine, 138 (2), 117–142.

[54] Yılmaz, Y., Genç, S.¸C., Gürer, F., Bozcu, M., Yılmaz, K., Karacık, Z., Altunkaynak, S., Elmas, A., (2000), When did the Western Anatolian grabens begin to develop? In: Bozkurt, E., Winchester, J.A., Piper, J.A.D. (eds) Tectonics and magmatism in Turkey and the surrounding area, Journal of the Geological Society of London, 173, 131–162.

[55] Ersoy, Y., Helvacı, C., (2007), Stratigraphy and geochemical features of the Early Miocene bimodal (ultrapotassic and calc-alkaline) volcanic activity within the NE-trending Selendi basin, western Anatolia, Turkey, Turkish Journal of Earth Sciences, 16, 117–139.

[56] Ersoy, E.Y., Helvacı, C., Palmer, M.R., (2011), Stratigraphic, structural and geochemical features of the NE-SW trending Neogene volcanosedimentary basins in western Anatolia: implications for associations of supradetachment and transtensional strike-slip basin formation in extensional tectonic setting, Journal of Asian Earth Sciences, 41, 159–183.

[57] Seyitoğlu, G., Anderson, D., Nowell, G., Scott, B.C., (1997), The evolution from Miocene potassic to Quaternary sodic magmatism in western Turkey: implications for enrichment processes in the lithospheric mantle, Journal of Volcanology and Geothermal Research, 76, 127–147.

[58] Çelik, Y., (1999), Sedimentology and coal-potantial of the Domaniç (Kütahya) Neogene basin, Dissertation, İstanbul University, İstanbul, 205 p.

[59] Özburan, M., Gürer, Ö.F., (2012), Late Cenozoic polyphase deformation and basin development, Kütahya region, western Turkey, International Geology Review, 54 (12), 1401-1418.

[60] Yağmurlu, F., Inaner, H., Nakoman, E., Inci, U., (2004), Age, tectonic setting, and quality distribution of the Neogene lignite deposits of western Anatolia, Geologica Belgica, 7 (3), 251−258.

[61] Ersoy, E.Y., Helvacı, C., (2016), Geochemistry and petrology of the lower Miocene bimodal volcanic units in the Tunçbilek–Domaniç basin, western Anatolia, International Geology Review, 58 (10), 1234-1252.

[62] Vassilev, S.V., Vassileva, C.G., Baxter, D., Andersen, L.K., (2010), Relationships between chemical and mineral composition of coal and their potential applications as genetic indicators. Part 2. Mineral classes, groups and species, Geologica Balcanica, 39 (3), 43–67.

[63] Vassilev, S., Vassileva, C., (1996), Mineralogy of combustion wastes from coal-fired power stations, Fuel Processing Technology, 47, 261–280.

[64] Ward, C.R., (2016), Analysis, origin and significance of mineral matter in coal: an updated review, International Journal of Coal Geology, 165, 1–27.

[65] Dai, S., Xie, P., Jia, S., Ward, C.R., Hower, H.C., Yan, X., French, D., (2017), Enrichment of U-Re-V-Cr-Se and rare earth elements in the Late Permian coals of the Moxinpo Coalfield, Chongqing, China: genetic implications from geochemical and mineralogical data, Ore Geology Review, 80, 1–17.

[66] Baş, H., (1983), Domaniç-Tavşanlı-Kütahya-Gediz yörelerinin Tersiyer jeolojisi ve volkanitlerinin petrolojisi, MTA Report No. 7293, 86 p.

[67] Türkmenoğlu, A.G., Yavuz-Işık, N., (2008), Mineralogy, chemistry and potential utilization of clays from coal deposits in the Kütahya province, Western Turkey, Applied Clay Science, 42, 63-73.

[68] Fu, X., Wang, J., Tan, F., Feng, X., Zeng, S., (2013), Minerals and potentially hazardous trace elements in the late Triassic coals from the Qiangtang Basin, China, International Journal of Coal Geology, 116-117, 93–105.

[69] Wang, X., Wang, X., Pan, S., Yang, Q., Hou, S., Jiao, Y., Zhang, W., (2018), Occurrence of analcime in the middle Jurassic coal from the Dongsheng Coalfield, northeastern Ordos Basin, China, International Journal of Coal Geology, 196, 126–138.

[70] Finkelman, R.B., Palmer, C.A., Wang, P., (2018), Quantification of modes of occurrence of 42 elements in coal, International Journal of Coal Geology, 185, 138–160.

[71] Hayashi, K.I., Fujisawa, H., Holland, H.D., Ohmoto, H., (1997), Geochemistry of ~1.9 Ga sedimentary rocks from northeastern Labrador, Canada, Geochimica Cosmochimica Acta, 61, 4115–4137.

[72] He, B., Xu, Y.G., Zhong, Y.T., Guan, J.P., (2010), The Guadalupian–Lopingian boundary mudstones at Chaotian (SW China) are clastic rocks rather than acidic tuffs: implication for a temporal coincidence between the end-Guadalupian mass extinction and the Emeishan volcanism, Lithos, 119, 10–19.

[73] Dai, S., Yang, J., Ward, C.R., Hower, J.C., Liu, H., Garrison, T.M., French, D., O'Keefe, J.M.K., (2015b), Geochemical and mineralogical evidence for a coal-hosted uranium deposit in the Yili Basin, Xinjiang, northwestern China, Ore Geology Review, 70, 1–30.

[74] Dai, S., Seredin, V.V., Ward, C.R., Hower, J.C., Xing, Y., Zhang,W., Song,W.,Wang, P., (2015c), Enrichment of U–Se–Mo–Re–V in coals preserved within marine carbonate successions: geochemical and mineralogical data from the Late Permian Guiding Coalfield, Guizhou, China, Mineralium Deposita, 50, 159–186.

[75] Ketris, M.P., Yudovich, Y.E., (2009), Estimations of Clarkes for carbonaceous biolithes: world average for trace element contents in black shales and coals, International Journal of Coal Geology, 78, 135–148.

[76] Dai, S., Wang, P., Ward, C.R., Tang, Y., Song, X., Jiang, J., Hower, J.C., Li, T., Seredin, V.V., Wagner, N.J., Jiang, Y.,Wang, X., Liu, J., (2015a), Elemental and mineralogical anomalies in the coal-hosted Ge ore deposit of Lincang, Yunnan, southwestern China: key role of N_2–CO_2-mixed hydrothermal solutions, International Journal of Coal Geology, 152, 19–46.

[77] Finkelman, R.B., (1981), Modes of occurrence of trace elements in coal: USGS Open-File Report No. OFR-81–99, 301 p.

[78] Finkelman, R.B., (1988), The inorganic geochemistry of coal: a scanning electron microscopy view, Scanning Microscopy, 2 (1), 97-105.

[79] Finkelman, R.B., (1994), Modes of occurrence of potentially hazardous elements in coal: levels of confidence, Fuel Processing Technology, 39, 21–34.

[80] Rudnick, R.L., Gao, S. (2003), Treatise on geochemistry, volume 3, In: The Crust, Holland, H.D. and Turekian, K.K. (Eds), Elsevier-Pergamon, Oxford, 683 p.

[81] Dai, S., Ji, D., Ward, C.R., French, D., Hower, J.C., Yan, X., Wei, Q., (2018b), Mississippian anthracites in Guangxi Province, southern China: Petrological, mineralogical, and rare earth element evidence for high-temperature solutions. International Journal of Coal Geology, 197, 84–114.

[82] Jones, B., Manning, D.A.C., (1994), Comparison of geochemical indices used for the interpretation of palaeoredox conditions in ancient mudstones. Chemical Geology, 111, 111–129.

[83] Karadirek, S., Altunsoy, M., (2022), Geochemical characteristics and paleodepositional setting of coal-bearing strata in Konya-Karapınar Basin, Central Anatolia, Turkey. Journal of African Earth Sciences, 186, 1-13.

[84] Galarraga, F., Reategui, K., Martinez, A., Martinez, M., Llamas, J.F., Marquez, G., (2008), V/Ni ratio as a parameter in palaeoenvironmental characterisation of non-mature medium crude oils from several Latin American basins. Journal of Petroleum Science and Engineering, 61, 9–14.

[85] El-Sabagh, S.M. Rashad, A.M. El-Naggar, A.Y. El Nady, M.M. Badr, I.A. Ebiad M.A., Abdullah E.S., (2018), API gravities, vanadium, nickel, sulfur, and their relation to gross composition: Implications for the origin and maturation of crude oils in Western Desert, Egypt, Petroleum Science and Technology, 36, 1-8.

[86] Kimura, H., Watanabe, Y., (2001), Ocean anoxia at the Precambrian–Cambrian boundary. Geology, 29, 995–998.

[87] Shi, L., Feng, Q.L., Shen, J., Ito, T., Chen, Z.Q., (2016), Proliferation of shallow-water radiolarians coinciding with enhanced oceanic productivity in reducing conditions during the Middle Permian, South China: evidence from the Gufeng Formation of western Hubei Province. Paleogeography, Paleoclimatology, Paleoecology, 444, 1–14.

[88] Lerman, A., Imboden, D.M., Gat, J.R., (1995), Physics and Chemistry of Lakes. Springer, Berlin, Heidelberg.

[89] Roy, D.K., Roser, B.P., (2013), Climatic control on the composition of Carboniferous–Permian Gondwana sediments, Khalaspir basin, Bangladesh. Gondwana Research, 23, 1163–1171.

[90] Finkelman, R.B., (1993), Trace and minor elements in coal, In: Organic Geochemistry Engel, M.H., Macko, S.A. (Eds), Plenum, New York, pp. 593–607.

[91] Dai, S., Zhou, Y., Ren, D., Wang, X., Li, D., Zhao, L., (2007), Geochemistry and mineralogy of the Late Permian coals from the Songzao Coalfield, Chongqing, southwestern China, Science In China Series D-Earth Sciences, 50, 678–688.

[92] Yalçın Erik, N., (2022), A non-traditional resource for critical minerals; Rare Earths (REY+Sc) contents of some Turkish low rank coals, Kahramanmaras Sutcu Imam University Journal of Engineering Sciences, 25, 155-172.

[93] Taylor, S.R., McLennan, S.H., (1985), The continental crust: Its composition and evolution, Blackwell, Oxford, 312 p.

[94] Dai, S., Graham, I.T., Ward, C.R., (2016), A review of anomalous rare earth elements and yttrium in coal, International Journal of Coal Geology, 159, 82–95.

[95] Yan, X., Dai, S., Graham, I.T., He, X., Shan, K., Liu, X., (2018), Determination of Eu concentrations in coal, fly ash and sedimentary rocks using a cation exchange resin and inductively coupled plasma mass spectrometry (ICP-MS), International Journal of Coal Geology, 191, 152–156.

[96] Yan, X., Dai, S., Graham, I.T., French, D., (2019), Mineralogy and geochemistry of the Palaeogene low-rank coal from the Baise Coalfield, Guangxi Province, China: Contributions from surrounding terrigenous lithologies and the depositional environment, International Journal of Coal Geology, 214, 103282.

[97] Dai, S., Ren, D., Chou, C.-L., Li, S., Jiang, Y., (2006), Mineralogy and geochemistry of the No. 6 coal (Pennsylvanian) in the Junger Coalfield, Ordos Basin, China. International Journal of Coal Geology, 66, 253–270.

[98] Bau, M., Koschinsky, A., Dulski, P., Hein, J.R., (1996), Comparison of the partitioning behaviours of yttrium, rare earth elements, and titanium between hydrogenetic marine ferromanganese crusts and seawater. Geochimica Cosmochimica Acta, 60, 1709–1725.